Current distribution effects in magnetoresistive tunnel junctions

Current distribution effects in magnetoresistive tunnel junctions

R. J. M. van de Veerdonk[a)]
Department of Applied Physics and COBRA, Eindhoven University of Technology, P.O. Box 513, 5600 MB Eindhoven, The Netherlands and Francis Bitter Magnet Laboratory, Massachusetts Institute of Technology, Cambridge, Massachusetts 02319

J. Nowak, R. Meservey, and J. S. Moodera
Francis Bitter Magnet Laboratory, Massachusetts Institute of Technology, Cambridge, Massachusetts 02319

W. J. M. de Jonge
Department of Applied Physics and COBRA, Eindhoven University of Technology, P.O. Box 513, 5600 MB Eindhoven, The Netherlands

(Received 28 July 1997; accepted for publication 12 September 1997)

The influence of an inhomogeneous current density on the (magneto)resistance of a ferromagnet–insulator–ferromagnet tunnel junction in the cross-strip geometry is analyzed using a finite element approach. The four-probe resistance is smaller than the actual resistance for electrode resistances (in the junction area) comparable to or higher than the junction resistance. Even negative four-probe resistances can be obtained. The apparent resistance change due to the junction magnetoresistive effect also decreases, but always remains positive. This results in unrealistically large apparent magnetoresistance ratios which can even approach infinity, which explains some recent experiments. © *1997 American Institute of Physics.* [S0003-6951(97)03245-2]

Tunnel junctions consisting of two ferromagnetic layers separated by a thin insulating layer show large magnetoresistive effects when the magnetizations of the ferromagnetic layers change their relative orientation from parallel to antiparallel in an applied magnetic field.[1,2] This result has attracted considerable attention due to its potential applicability in low power magnetic field sensors or nonvolatile memory devices. The largest magnetoresistive effects have been observed in low resistance junctions (compared to the lead resistance in the same area). Low resistances can in some cases be explained by a large surface area (i.e., scaling effect) or by a low tunnel resistivity (i.e., barrier property). Moodera *et al.*[3] observed that by reducing the barrier resistivity the magnetoresistance ratio, defined as the resistance change divided by the resistance in a reference state, increased to significantly higher values for otherwise identical junctions. This was qualitatively attributed to the measuring geometry artifact described here. Similarly, Kamugai *et al.*[4] observed that for microfabricated junctions the magnetoresistance ratio is smaller than for similar macroscopic junctions.[2]

Most results up to now are obtained with the tunnel junctions in the cross-strip geometry, shown schematically in Figure 1. Two (ferromagnetic) electrodes are configured perpendicular to each other and are separated by an insulating layer; the intersection defines the junction area. The four-probe resistance is measured by sending a current using one of the facing contacts on each electrode and measuring the voltage difference between the other two. Resistance measurements in similar geometries[5–7] are known to cause problems due to inhomogeneous current distribution effects when the electrode resistances (in the same area) become comparable to the perpendicular resistance. The four-probe resistance appears to be lower than expected, and even negative resistances have been found. Qualitatively explanations have been proposed[5–7] based on one dimensional (1D) analytical models taking into account the electrode resistances. However, to the best of our knowledge no analytical solutions exist for the current distribution in the cross-strip geometry. Also the effect on magnetoresistive properties is not accounted for in previous models. Therefore, we performed finite element calculations taking into account the whole geometry.

In order to calculate the four-probe resistance, we model the junction by two perpendicular stripes extending some distance outside the junction area (see Figure 1). Perpendicular current flow within the electrodes is neglected. The current distribution within the bottom electrode is governed by Ohm's law:

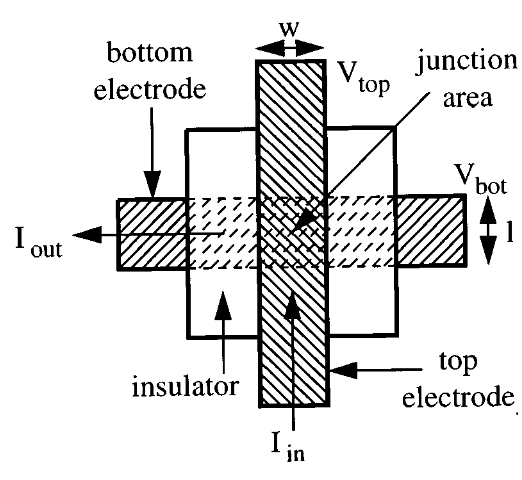

FIG. 1. Schematic of the cross-strip geometry. The junction area is defined as the intersection of the two perpendicular electrodes (hatched), which are separated by a thin insulating layer.

[a)]Postal address: Philips Research Laboratories, Prof. Holstlaan 4, 5656 AA Eindhoven, The Netherlands.
Electronic mail: veerdonk@natlab.research.philips.com

$$\mathbf{j}_b = -\rho_b^{-1} \nabla V_b , \tag{1}$$

where $\mathbf{j}_b$ is the local in-plane current density, ρ_b the resistivity, and V_b the local voltage in the bottom electrode. From current conservation we find:

$$d_b \nabla \cdot \mathbf{j}_b + j_{\mathrm{tun}} = 0 , \tag{2}$$

where d_b is the thickness of the bottom electrode, and j_{tun} is the local tunnel current density. Similar equations hold for the top electrode. The tunnel current is modelled as:

$$j_{\mathrm{tun}} = \rho_j^{-1} (V_b - V_t) , \tag{3}$$

where ρ_j is the tunnel resistivity in Ω m^2, which in general depends on the voltage difference between the top and bottom electrode. In the present case, we restrict the calculations to the linear (low voltage) regime, although the inclusion of nonlinear effects is straightforward.

By substituting these equations we find two coupled equations for the voltage distributions in the top and bottom electrodes:

$$\frac{\partial^2 V_{b(t)}}{\partial x^2} + \frac{\partial^2 V_{b(t)}}{\partial y^2} = \frac{R_{\Box,b(t)}}{\rho_j} (V_{b(t)} - V_{t(b)}) , \tag{4}$$

where $R_{\Box,b(t)} = \rho_{b(t)} / d_{b(t)}$ is the square resistance of the bottom (top) electrode. The only free parameter in this equation is the ratio between the square resistance of the electrodes and the tunnel resistivity. This parameter can be written as:

$$\frac{\rho_j}{R_{\Box,b(t)}} = l_{\mathrm{typ}}^2 = \frac{R_j}{R_{b(t)}} w^2 (l^2) , \tag{5}$$

where l_{typ} is the typical length scale of the current distribution, R_j and $R_{b(t)}$ are the expected resistances of the junction and the electrodes (within the junction area), respectively, for a junction area with length l and width w. When the typical length scale $l_{\mathrm{typ}} < l, w$ or, alternatively, when the junction resistance $R_j < R_{b(t)}$, the current density distribution will become inhomogeneous.

A finite element approach is used to solve Equation (4). As boundary conditions a voltage of ± 1 V at the end of each of the current leads is used. An example of the calculated potential and tunnel current density distributions within the junction area are shown in Figure 2. Both leads have a square resistance of $R_\Box = 20\ \Omega$, the junction area is a square with 200 μm sides, and the tunnel resistivity ρ_j is chosen such that the actual junction resistance equals the resistance of the electrodes. The voltage distribution for the bottom electrode is not shown for this symmetric junction. As can be seen the in-plane voltage drop within the junction area is significant and as a result the tunnel current is largest in the corner where both current leads meet (i.e., the current takes the shortest path). Since the voltages are measured at the other sides, the apparent junction resistance is smaller than the actual junction resistance.

The four-probe resistance R_{4p} can be calculated similar to the experiment by dividing the voltage difference in the voltage leads by the total tunnel current. In Figure 3 $R_{4\mathrm{p}}$ and $\Delta R_{4\mathrm{p}}$ due to a small magnetoresistive change in the tunnel resistivity are shown for varying ρ_j. Both quantities are scaled to the actual values for the junction resistance R_j and

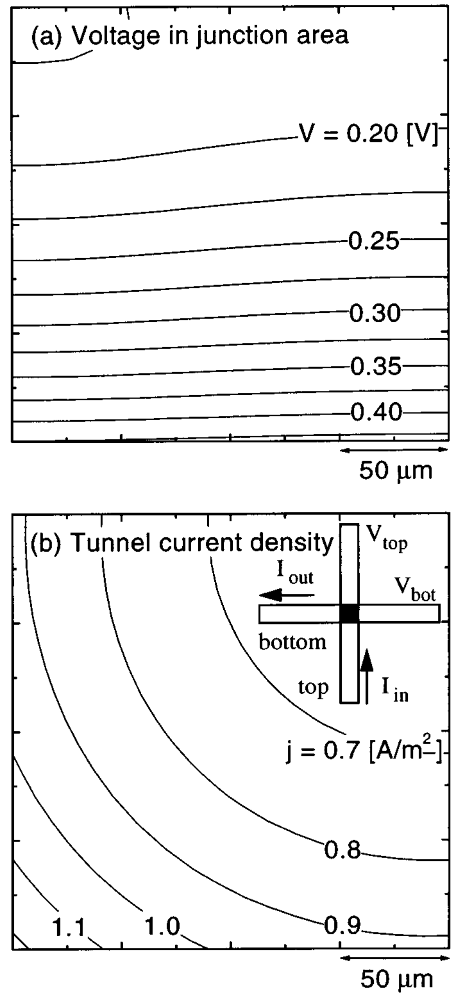

FIG. 2. (a) The calculated voltage distribution in the top electrode for a junction with $l_{\mathrm{typ}} (= l, w) = 200\ \mu$m ($R_j = R_{b(t)} = 20\ \Omega$). (b) The tunnel current density distribution shows an increased current density in the corner where the current leads meet. Only the junction area is shown.

junction resistance change ΔR_j. As shown in Figure 3(a), a considerable reduction of the scaled four-probe resistance occurs for $R_j < R_{b(t)}$ or, alternatively, for $l_{\mathrm{typ}} < l, w$. Also the scaled four-probe resistance change shows a reduction, as shown in Figure 3(b). However, its value always remains positive. This can be understood when this quantity is viewed as a (scaled) derivative with respect to R_j of the four-probe resistance, which shows a monotonic behavior. Combined, these effects lead to an infinite apparant magnetoresistance ratio at the point where the apparent junction resistance in the reference state approaches zero.

Using the approach described above, the experiments reported in Refs. 2 and 3 have been reinterpreted by modeling the four-probe resistances in the parallel and antiparallel states, using only the tunnel resistivity as a parameter. For the 10 Ω junction in Figure 2(a) of Ref. 3, a corrected magnetoresistance ratio of 19% is found (relative to the high resistance state) instead of the 30% obtained from the measurement. The corrected value is consistent with the values obtained for high resistance junctions.[1,8] For the junction with the negative resistance of Figure 2(c) of Ref. 3 a corrected value of 15% is found, compared to the observed value of over 1000% (relative to the high resistance state).

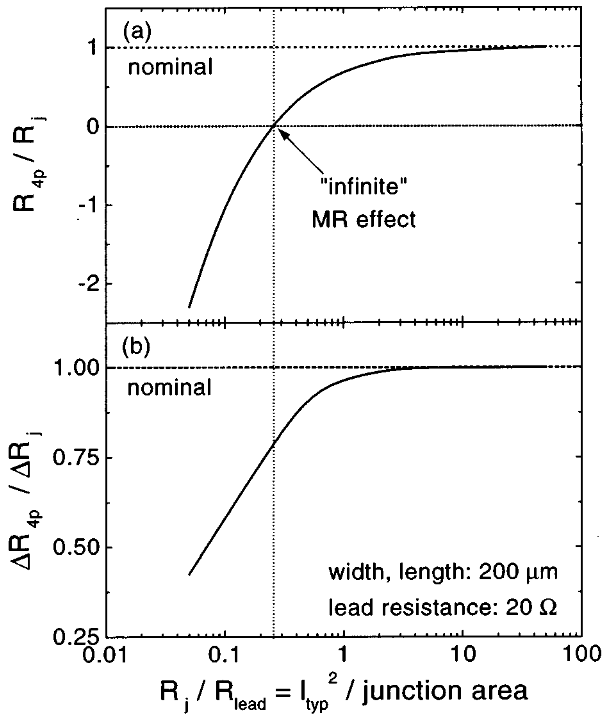

FIG. 3. The calculated (a) scaled four-probe resistance R_{4p}/R_j and (b) scaled resistance change $\Delta R_{4p}/\Delta R_j$ for a junction with $l,w=200$ μm, $R_{b(t)}=20$ Ω, with varying ρ_j.

Also for this junction the corrected value is more in line with the results obtained for higher resistance junctions.[1,8]

Similarly, for the data presented in Figure 1 of Ref. 2 for a 1 mm^2 area tunnel junction with a 7 mΩ resistance we find a corrected magnetoresistance ratio of 1.2%, much reduced from the measured 18% (relative to the low resistance state). Recently, new measurements have been presented by this group on microfabricated tunnel junctions (where $l_{typ} > l,w$) with magnetoresistance ratios of a few tenths of a percent.[4] Also in this case the corrected value is more in line with the data for junctions without the inhomogeneous current distribution effect (in this case by reducing the area).

In conclusion, we would like to state that care should be taken when comparing experimentally obtained data on magnetoresistive tunnel junctions. The measurements for low resistance junctions should be corrected for inhomogeneous current distribution effects. It should be noted that the apparent enhancement of the magnetoresistance ratio does not lead to increased application potential, since the actual resistance change (and hence the signal) is reduced. The inhomogeneous current distribution effects occur for junctions with resistances of the electrodes (in the junction area) comparable to or higher than the junction resistance or, similarly, when the typical length scale of the effect becomes smaller than the junction dimensions. Problems can be avoided by increasing the tunnel resistivity, decreasing the junction dimensions, or lowering the electrode resistances by adding well conducting layers.

R.V. acknowledges a travel grant from the Dutch Technology Foundation (NWO). J.N. is an IBM Research Partnership Award postdoctoral fellow. This work was supported in part by the EUT/Philips Research collaboration, ESPRIT Research Project No. 20 027, ''Novel Magnetic Nanodevices of artificially layered Materials (NM)^2,'' NSF Grant No. DMR 9423013, and ONR Grant No. N00014-92-J-1847.

[1] J. S. Moodera, L. R. Kinder, T. M. Wong, and R. Meservey, Phys. Rev. Lett. **74**, 3273 (1995); J. S. Moodera and L. R. Kinder, J. Appl. Phys. **79**, 4724 (1996).
[2] T. Miyazaki and N. Tezuka, J. Magn. Magn. Mater. **139**, L231 (1995).
[3] J. S. Moodera, L. R. Kinder, J. Nowak, P. LeClair, and R. Meservey, Appl. Phys. Lett. **69**, 708 (1996).
[4] S. Kamugai, T. Yaoi, and T. Miyazaki, J. Magn. Magn. Mater. **166**, 71 (1997); T. Miyazaki, S. Kamugai, and T. Yaoi, J. Appl. Phys. **81**, 3753 (1997).
[5] I. Giaever, *Tunneling Phenomena in Solids*, edited by Burnstein (1967), p. 27.
[6] P. J. Pedersen and F. L. Vernon, Appl. Phys. Lett. **10**, 29 (1967).
[7] S. K. J. Lenczowski, R. J. M. van de Veerdonk, M. A. M. Gijs, J. B. Giesbers, and H. H. J. M. Janssen, J. Appl. Phys. **75**, 5154 (1994).
[8] J. S. Moodera (unpublished).